X-Ray Spectrometry

WILEY

X-RAY SPECTROMETRY

RESEARCH ARTICLE OPEN ACCESS

Evaluating the Microstructure and Interaction of Bioaggregates in Concrete Using microCT

Olga M. O. de Araujo[1] | Caio M. S. F. F. dos Santos[1] | Davi F. de Oliveira[1] | Rodolfo G. M. de Andrade[2] | Saulo R. Ferreira[3] | Ricardo T. Lopes[1]

[1]Universidade Federal do Rio de Janeiro (UFRJ), Rio de Janeiro, RJ, Brazil | [2]Civil Engineering and Buildings Department, Federal Institute of Espírito Santo, Vitória, ES, Brazil | [3]Federal University of Lavras, Lavras, MG, Brazil

Correspondence: Olga M. O. de Araujo (olgaufrjlin@gmail.com)

Received: 29 May 2025 | **Revised:** 23 September 2025 | **Accepted:** 1 October 2025

Funding: This study was financed in part by FAPERJ—Fundação Carlos Chagas Filho de Amparo à Pesquisa do Estado do Rio de Janeiro, through the Pós-Doutorado Nota 10 Fellowship (Grant No. SEI-260003/001101/2025 to O.M.O.A.), the National Council for Scientific and Technological Development—CNPq, INCT-INAIS (grant 406303/2022-3 and productivity fellowships 314225/2021 to R.T.L.).

Keywords: biomass | cementitious composites | MicroCT

ABSTRACT

This study investigates the use of x-ray computed microtomography (microCT) to evaluate the incorporation of bioaggregates—specifically macauba *(Acrocomia aculeata)* endocarp and jute fibers—into cement-based composites. MicroCT enables non-destructive, three-dimensional characterization of the internal microstructure, providing insights into the spatial distribution of the bioaggregates and their interaction with the cementitious matrix. This study evaluates the influence of bioaggregate incorporation on the composite. Additionally, considering the high-energy demands of the construction sector, the integration of sustainable materials such as bioaggregates and phase change materials (PCMs) is explored as a strategy to enhance energy efficiency and reduce environmental impact. The findings demonstrate the potential of bioaggregates to contribute to more eco-friendly construction materials and underscore the value of advanced imaging techniques in sustainable materials research.

1 | Introduction

The construction industry is one of the most resource-intensive sectors globally, accounting for a substantial portion of natural resource consumption and greenhouse gas emissions [1]. In response to increasing environmental concerns, the development of sustainable construction materials has gained momentum. Among the strategies explored, the incorporation of bioaggregates—agricultural by-products such as plant fibers, shells, and seed endocarps—has emerged as a viable strategy to reduce dependency on non-renewable resources while improving the ecological profile of cementitious composites [2].

Notably, jute fibers and the endocarp of macauba *(Acrocomia aculeata)* have attracted attention due to their mechanical strength, thermal insulation capacity, biodegradability, and regional availability in tropical areas [3]. These bioaggregates contribute to improved sustainability without compromising performance and have demonstrated potential in reinforcing cement-based matrices [4, 5]. However, their successful application requires careful investigation of their interaction with the matrix, moisture sensitivity, and influence on the hydration process [6].

One of the most effective approaches for characterizing such composites is x-ray computed microtomography (microCT), a non-destructive 3D imaging technique that provides high spatial resolution and volumetric data. Unlike traditional destructive or surface-limited methods, microCT enables internal visualization of bioaggregate distribution, pore networks, and interfacial bonding with the cementitious matrix [7]. This capability is essential for identifying weak zones, air voids,

This is an open access article under the terms of the Creative Commons Attribution License, which permits use, distribution and reproduction in any medium, provided the original work is properly cited.

© 2025 The Author(s). *X-Ray Spectrometry* published by John Wiley & Sons Ltd.

and heterogeneities that affect durability and mechanical performance [8]. Moreover, microCT facilitates the study of degradation mechanisms such as fiber debonding and moisture ingress, which are critical for predicting long-term behavior [9].

The demand for multifunctional construction materials has also led to interest in composites that integrate phase change materials (PCMs), which enhance thermal performance by regulating temperature fluctuations inside buildings. PCMs, combined with bioaggregates, may synergistically improve energy efficiency and material performance, though their microscale interactions and effects on cement hydration, and mechanical properties are underexplored [10].

Recent studies have emphasized the role of nano-reinforcement strategies using cellulose microcrystals and nanofibrils to improve fiber-matrix interfaces [11]. Likewise, microCT has proven effective in studying the mechanical integrity and distribution of natural aggregates in cementitious composites, making it a valuable tool for advancing sustainable material design [12].

This study aims to evaluate the spatial distribution and interfacial bonding of macauba endocarp and jute fibers within cement-based composites by employing high-resolution microCT. Through detailed 3D imaging, the research seeks to understand how these bioaggregates interact with the cementitious matrix at the microscale, with special attention to their arrangement, pore connectivity, and interface characteristics. Additionally, the study investigates the potential synergy between bioaggregates and phase change materials (PCMs), exploring how their integration can enhance the thermal and structural performance of sustainable construction materials. By combining advanced non-destructive imaging techniques with innovative bio-based formulations, this work contributes to the development of eco-efficient building composites aligned with global sustainability and energy efficiency.

2 | Materials and Methods

2.1 | Bioaggregates

The materials used in this study included bioaggregates, Type V-ARI cement from Mauá/LafargeHolcim (equivalent to European CEM I 52.5N) [13], mineral coarse aggregates (oblong-shaped crushed granite), and distilled water. The chemical composition of the cement is detailed in Table 1.

TABLE 1 | Description of the chemical composition of CPV-ARI cement.

Chemical and physical properties	Value
CaO (%)	63.8
SiO_2 (%)	17.8
SO_3 (%)	3.82
Al_2O_3 (%)	4.98
K_2O (%)	0.82
TiO_2 (%)	0.21
MnO (%)	0.10
Others (%)	8.47
Density (g/cm^3)	3.2
Superficial Area (m^2/kg)	420

The bioaggregates used in this study were derived from two natural sources: the Macauba fruit and jute fibers. One of the bioaggregates was obtained from the macauba fruit, which has two commercially valuable components—the pulp and the nut. After pulp extraction, the fruit undergoes high-speed centrifugation to separate the nut, and the remaining by-product, the crushed endocarp, is collected and used as a residue-based bioaggregate. Jute fibers, in turn, are extracted from the stem of the *Corchorus capsularis* plant through a sequence of cutting, retting, crushing, drying, packaging, and sorting processes [14], while the textile form is produced through spinning and weaving. The jute textile used in this work presents a mesh spacing of 3.5 yarns/cm in the longitudinal direction. To investigate the fiber–matrix interface, untreated and polymer-treated jute yarns extracted from this textile were embedded in cement paste matrices (water-to-cement ratio = 0.3). For image acquisition, individual yarns were inserted into 2 mL microcentrifuge tubes, which were then filled with cement paste. Figure 1 shows the bioaggregate samples used in this study: crushed macauba endocarp and jute yarn specimens embedded in cement.

2.2 | MicroCT

MicroCT scan analyses were conducted to investigate the internal structure and fiber–matrix interface of the bioaggregate samples. Two scanning protocols were employed, tailored to the specific characteristics of each material.

For the jute yarn specimens, the acquisition was performed using a Phoenix V|tome|x M system (Waygate Technologies, Wunstorf, Germany). Individual yarns were inserted into 2 mL microcentrifuge tubes, which were then filled with cement paste. The acquisition parameters for these samples included a voltage of 70 kV, a current of 280 μA, five frames per projection, an aluminum filter with a thickness of 0.5 mm, a magnification factor of 9.37, a pixel size of 21 μm, and a total of 1200 projections.

For the Macauba endocarp bioaggregate samples, the same microCT system was used with a different set of parameters to optimize resolution and contrast for the denser granular structure. The acquisition settings included a voltage of 100 kV, a current of 180 μA, an exposure time of 300 ms per projection, seven frames per projection, an aluminum filter with a thickness of 1 mm, a magnification factor of 10.43, pixel size and voxel size of 19 μm, and a total of 1500 projections.

All 3D reconstructions were carried out using the Phoenix Datos software (Waygate Technologies, Wunstorf, Germany),

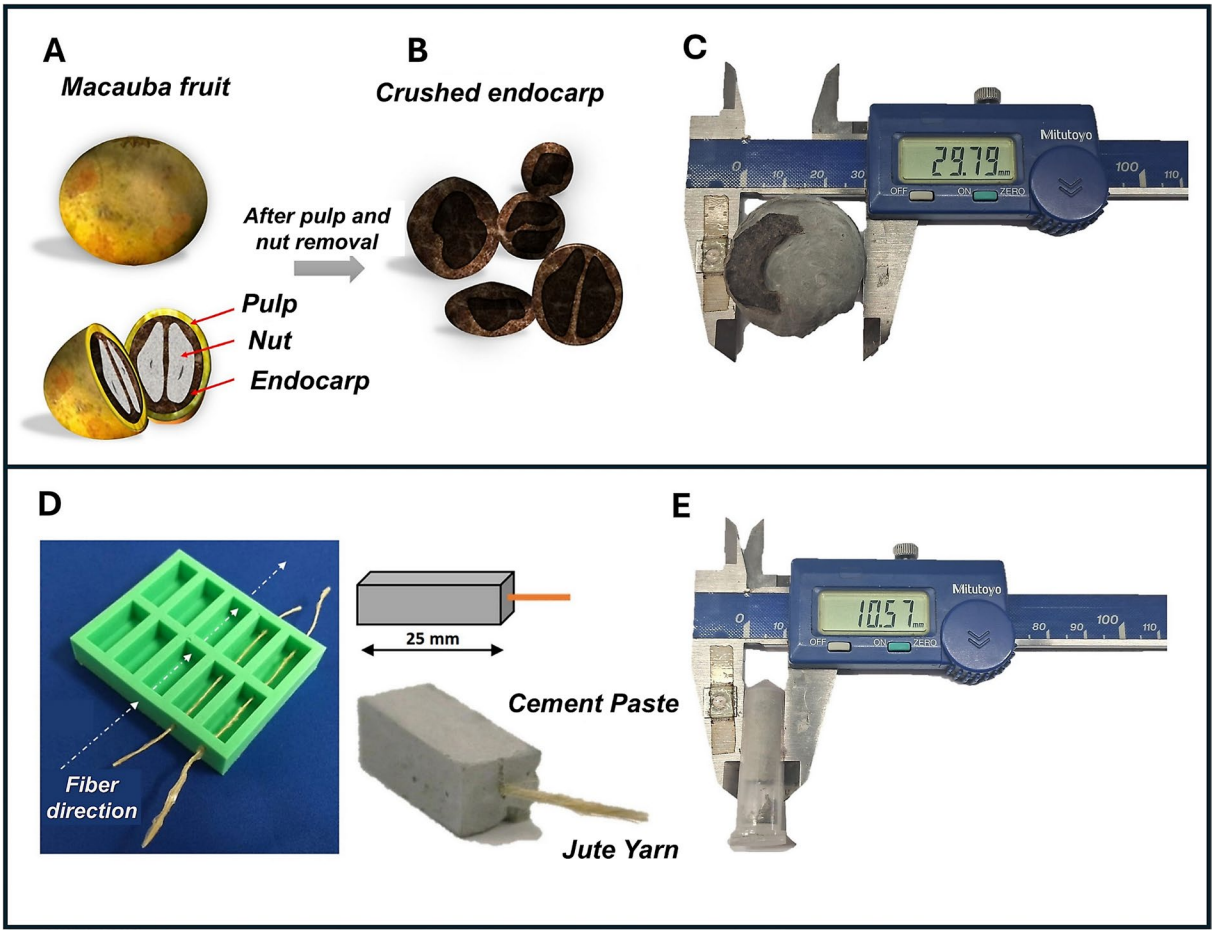


FIGURE 1 | Preparation of the bio-concrete samples. (A) Macauba fruit (*Acrocomia aculeata*), indicating its main components: pulp, nut, and endocarp. (B) Crushed endocarp obtained after pulp and nut removal through mechanical centrifugation. (C) Bio-concrete with crushed endocarp particles. (D) Jute yarn samples extracted from textile fabric and embedded in cement paste molds for mechanical testing. (E) Bio-concrete with jute yarn sample. [Colour figure can be viewed at wileyonlinelibrary.com]

where slice alignment, beam hardening correction, and a mathematical edge-enhancement filter were applied to improve contrast between the matrix and pore spaces. For visualization and further analysis of 2D and 3D data, VG Studio Max v. 3.0 (Volume Graphics GmbH, Heidelberg, Germany) was used.

2.3 | Deep Learning Segmentation

To optimize the analysis of the interfacial regions and internal structure of the cementitious composite, a deep learning-based approach was implemented using the Deep Learning Segmentation (DLS) module in VGStudio MAX. This method was a core step in the image processing workflow, enabling the precise classification of complex phases, unlike classical segmentation techniques that rely solely on grayscale thresholds. The workflow was structured into the following steps: First, a training dataset was created directly from the reconstructed 3D volumes of the scanned samples. Representative 2D slices were selected from across the volumes, and three primary phases were manually labeled to create precise segmentation masks: bioaggregates, cement matrix, and pores. The training set was composed of 6000 slices in total, providing a comprehensive basis for the network to learn the specific microstructural features of the composites under study.

These annotated slices were then used to train a convolutional neural network (CNN) within the software. The training process allowed the algorithm to learn subtle morphological patterns and textural cues essential for differentiating the phases, particularly in low-contrast zones such as the bioaggregate-matrix interface. Once trained, the model was applied to the entire 3D datasets, resulting in a consistent and robust segmentation across all slices, even in areas with signal noise or grayscale overlap.

The performance of this deep learning methodology was evaluated by its ability to overcome the limitations of conventional segmentation methods. A separate experimental validation with quantitative metrics was not performed, as a primary objective of this study was to demonstrate the effectiveness of this advanced segmentation approach compared to standard techniques (e.g., thresholding). The superiority of the deep learning method is thus demonstrated by the quality of the segmentation and the detailed microstructural findings presented in this work. This method proved especially effective for distinguishing features at the aggregate–matrix boundary, where standard segmentation

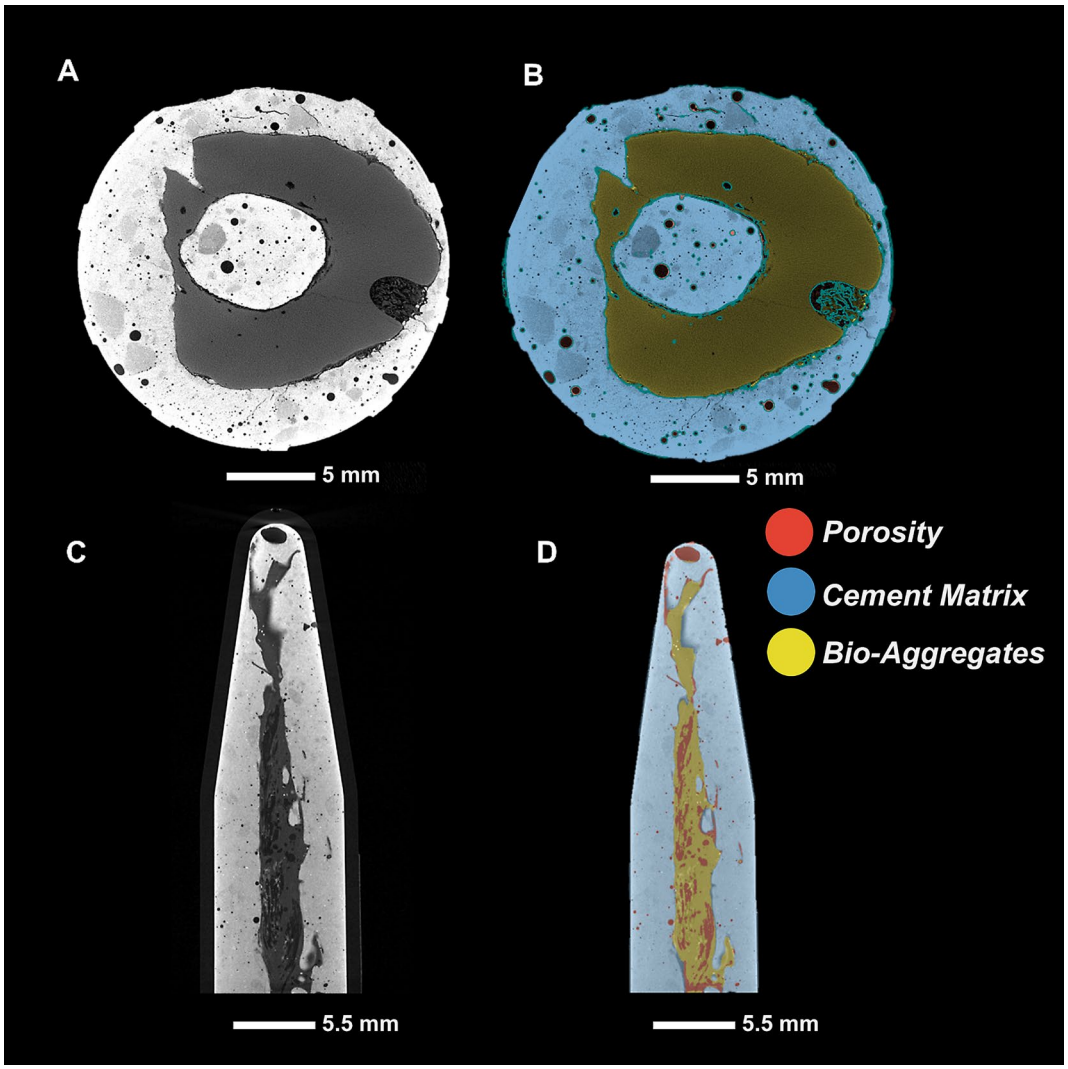


FIGURE 2 | Deep learning-based segmentation of cementitious samples with bio-aggregates. Images (A) and (C) show representative grayscale slices of samples containing macauba endocarp and jute fiber, respectively. The corresponding segmentation results are shown in (B) and (D) present the corresponding segmentation results, where the bio-aggregate phase is highlighted in yellow, the cementitious matrix in blue, and the pore space in red. This approach enables precise differentiation of phases and improved detection of interfacial porosity, particularly in low-contrast and heterogeneous regions. [Colour figure can be viewed at wileyonlinelibrary.com]

often underestimates porosity or misclassifies transition zones. As shown in Figure 2, the deep learning-based segmentation accurately isolates the bioaggregate, matrix, and pore phases, enabling a more detailed quantification of volume fractions and interfacial porosity.

3 | Results and Discussion

3.1 | Interfacial Analysis of the Macauba Endocarp Bioaggregate

To explore the nature of the bond between the macauba endocarp bioaggregate and the cementitious matrix, linear measurements were performed on reconstructed grayscale slices obtained via microCT as shown in Figure 3. These measurements focused on the interfacial transition zone (ITZ), a critical region for the mechanical performance and durability of bio-based cementitious composites [15, 16]. As the endocarp and the cement paste exhibit distinct densities, a clear contrast between both phases facilitated the delineation of the interface.

MicroCT analysis confirmed the absence of voids along the perimeter of the matrix–aggregate interface, indicating a strong and effective chemical interaction and a high degree of adhesion between phases. This behavior is indicative of a well-established interfacial bond, which may be attributed to the physicochemical compatibility between the rough, lignocellulosic surface of the endocarp and the hydration products of the cement [17]. Additionally, the observed interfacial configuration highlights mechanical interlocking and friction resulting from the bioaggregate's semi-ellipsoidal geometry and surface roughness, with tight bond distances measuring up to 0.51 mm (Figure 3B). Although adhesion appears consistent, zones of localized detachment, measuring up to 0.84 mm wide (Figure 3D), were occasionally identified, likely related to shrinkage effects during curing. Germination pores and internal channels in the

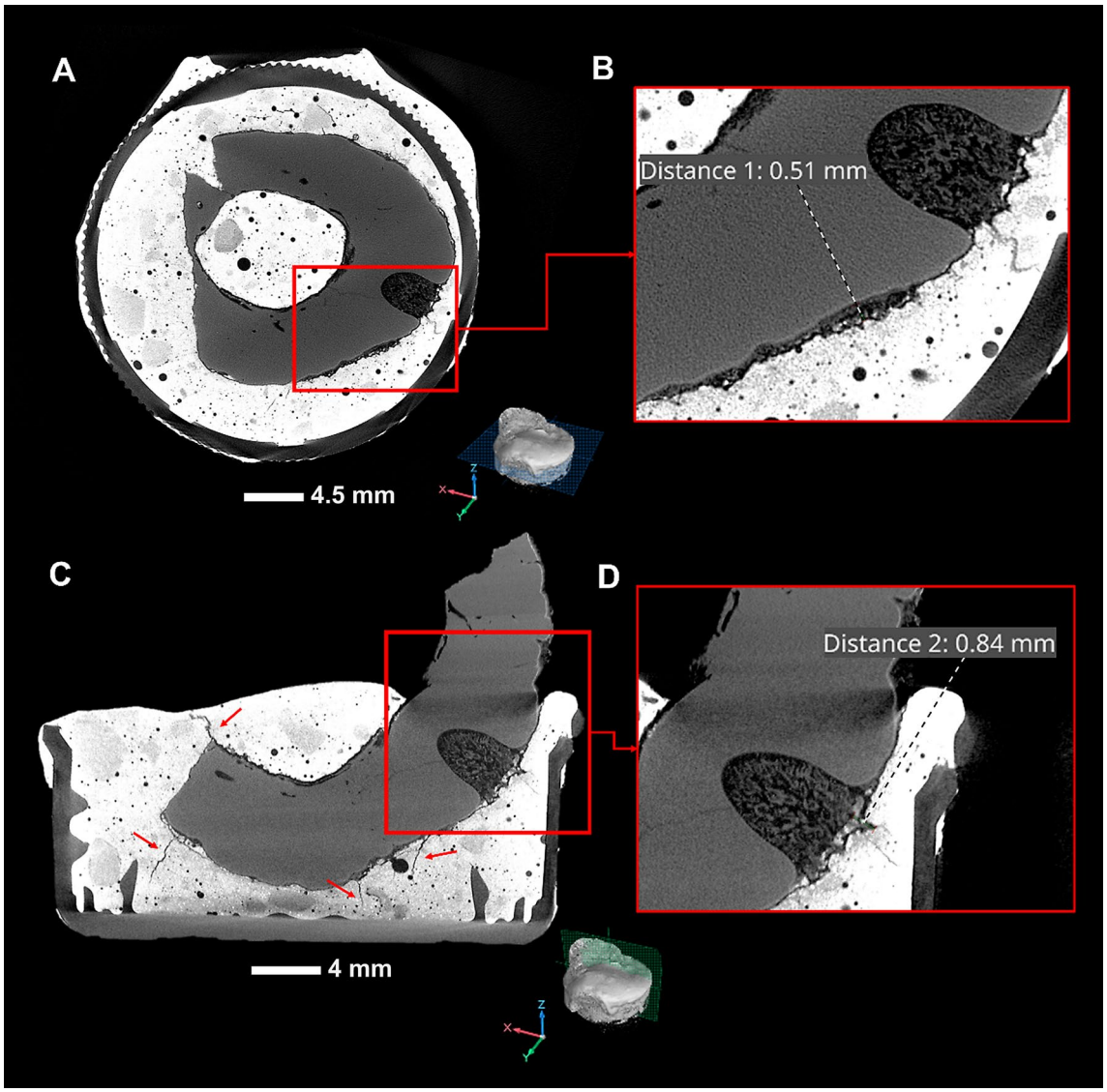


FIGURE 3 | Microstructural analysis of the interface between macauba endocarp and cementitious matrix. (A) Cross-section of the sample revealing the interfacial contact zone. (B) Details of the adhesion between the endocarp and the matrix. (C) Regions of localized detachment are attributed to shrinkage. (D) Detail of the mechanical interlocking facilitated by the roughness of the endocarp surface. [Colour figure can be viewed at wileyonlinelibrary.com]

endocarp structure were also visualized, providing further information on its porous morphology and potential water transport behavior.

These findings underscore microCT's capability to assess microstructural features at the bioaggregate–matrix interface, offering non-destructive information on bonding effectiveness and porosity distribution that would otherwise be difficult to evaluate.

Following the linear measurements of the interfacial region, volumetric analysis was performed to quantify the internal porosity and geometric characteristics of the macauba endocarp bioaggregate embedded in the cementitious matrix. The segmentation of the 3D dataset using deep learning algorithms enabled the isolation of distinct phases—bioaggregate, cement matrix, and pore spaces—facilitating precise calculation of structural parameters.

The macauba endocarp exhibited a total volume of 3504.24 mm^3 and a measured total porosity of 10.04%, concentrated predominantly in its internal structure. This porosity is associated with naturally occurring anatomical features such as germination pores and vascular channels, clearly visualized in the 3D volume rendering (see Figure 4D–F).

Figure 4A shows a 3D model of the segmented sample, with the cement matrix in translucent gray to reveal the color-coded pore distribution. Partial removal of the matrix in Figure 4B further emphasizes the porous structure. Analysis of the cement matrix revealed a total porosity of 15.75%, with pore diameters reaching up to 5 mm, as shown in the pore size distribution map in Figure 4C. These features are intrinsic to the material and contribute to its water absorption behavior and potential interaction with the matrix.

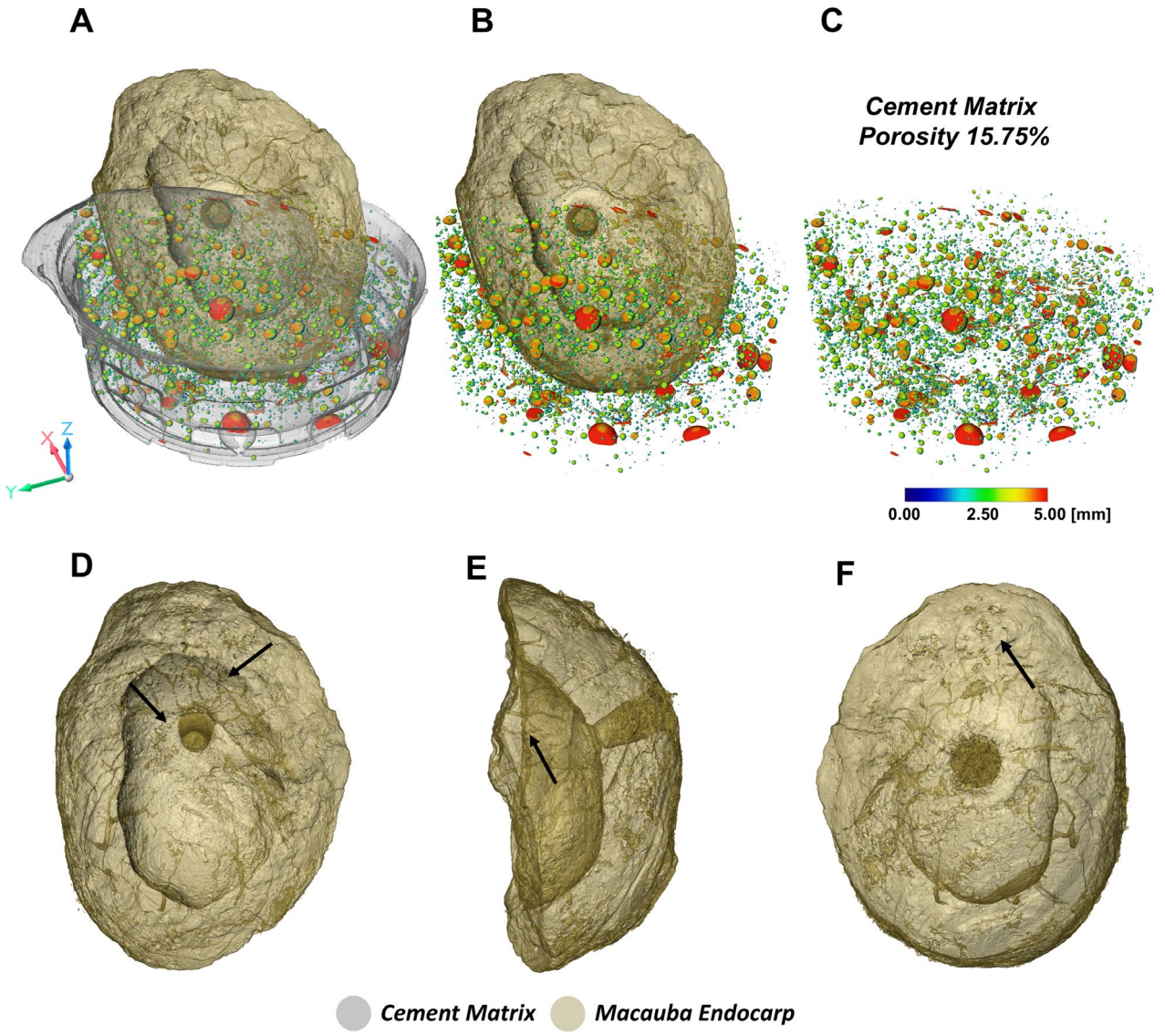


FIGURE 4 | Three-dimensional visualization of a cementitious composite sample containing macauba endocarp. (A) 3D model of the segmented sample, showing the cementitious matrix and pore distribution. (B) Visualization of the pore structure with the matrix visualization removed. (C) Pore size distribution map in the cementitious matrix. (D–F) Surface views of the macauba endocarp, showing its morphology with germination pores (arrows) and vascular channels. [Colour figure can be viewed at wileyonlinelibrary.com]

The relatively low porosity observed is advantageous in the context of cementitious composites, as it limits water uptake and shrinkage-induced detachment. Compared to other lignocellulosic bioaggregates, such as wood chips and straw, which often exhibit porosities exceeding 50%–70%, the macauba endocarp demonstrates improved dimensional stability. This bioaggregate absorbs ~9% of water by weight, which is significantly lower than typical values for wood-based materials (150%–200%), making it a more compatible and stable inclusion for cement-based formulations [17].

Moreover, the semi-ellipsoidal shape and irregular surface topology of the endocarp promote mechanical interlocking with the cement matrix, enhancing stress transfer at the interface. The combination of modest porosity, favorable geometry, and interfacial adhesion contributes to the potential of the macauba endocarp as an effective and sustainable reinforcement in bio-based concretes.

3.2 | Interfacial Analysis of the Jute Fiber Bioaggregate

The reconstructed microCT slices of the cementitious sample incorporating a single untreated jute yarn revealed distinct interfacial behavior compared to the macauba endocarp (Figure 5A). Linear measurements were performed at the fiber–matrix interface to assess the thickness of the interfacial transition zone (ITZ) and the extent of void formation. The average ITZ width measured ~115–160 μm, with localized regions exceeding 200 μm. The magnified view in Figure 5B reveals significant porosity and a maximum gap of 0.78 mm within the fiber bundle.

Unlike the endocarp, the jute yarn exhibited significant heterogeneity in matrix interaction. The outer filaments of the yarn were partially embedded in the cement paste, showing some degree of adhesion, whereas the inner filaments remained

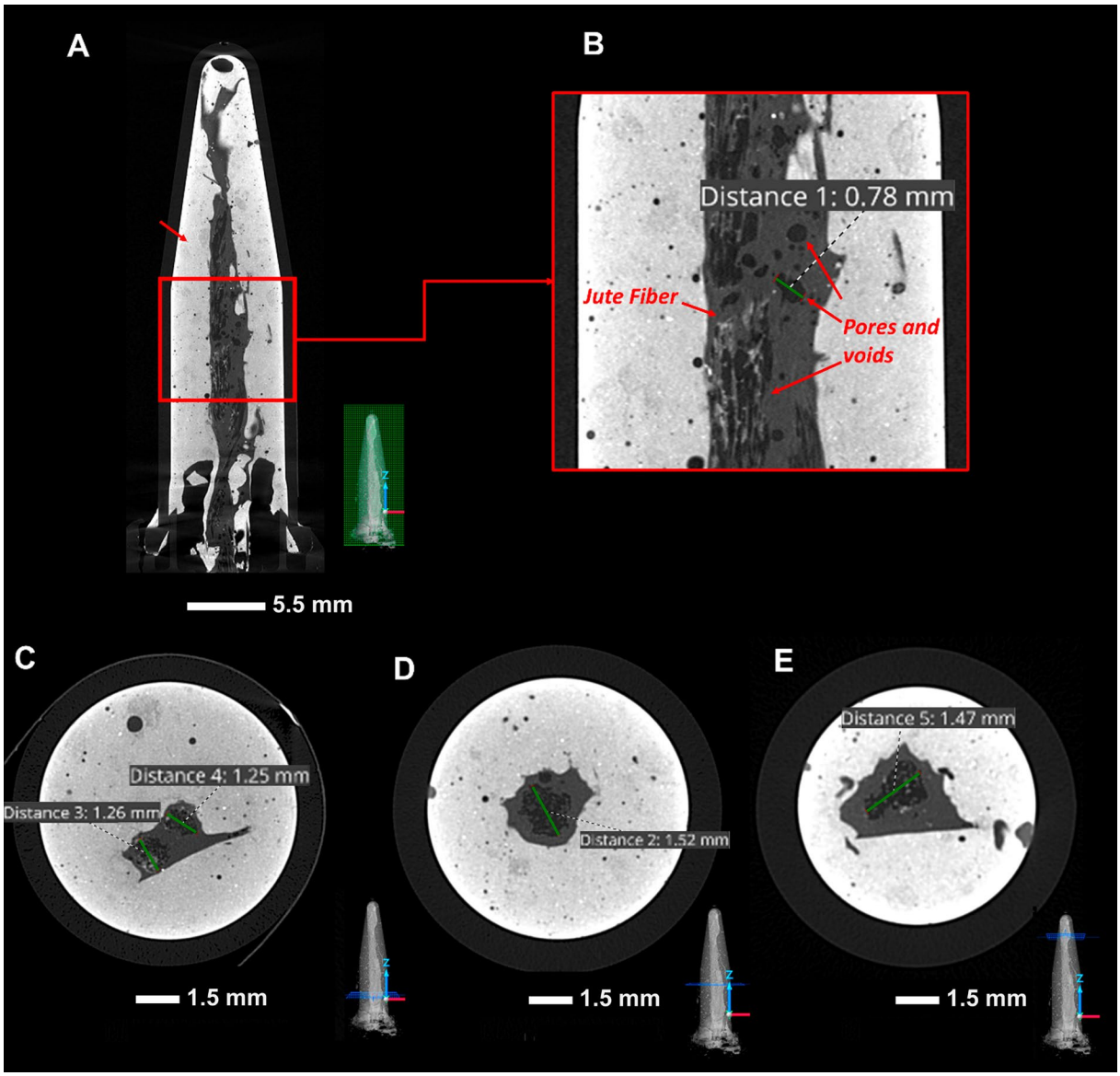


FIGURE 5 | Grayscale reconstructed sections highlighting the interface and interactions between the jute fiber and cement. (A) Longitudinal cross-section of the jute fiber bundle in the matrix. (B) Enlarged view showing the porosity and voids. (C–E) Cross-sections at different positions along the sample, showing the variable interaction within the jute yarn. [Colour figure can be viewed at wileyonlinelibrary.com]

unbonded, with visible air-filled gaps throughout the central region. Cross sections at different positions (Figure 5C–E) highlight this variable interaction, with linear measurements indicating internal diameters of 1.26, 1.25, 1.52, and 1.47 mm.

This lack of penetration by the cementitious matrix into the inner voids of the yarn can be attributed to the hydrophilic nature and high capillarity of the jute fibers, which tend to absorb water during curing and may promote localized shrinkage and debonding. Additionally, the untreated surface of the yarn lacks chemical compatibility with hydration products, limiting interfacial bonding.

These findings align with prior studies on natural fiber-reinforced cement composites, which report similar interfacial challenges due to fiber swelling, poor wetting, and limited paste infiltration [18]. The study highlighted that non-treated lignocellulosic fibers tend to form weak ITZs, often containing entrapped air and microcracks. The linear measurements obtained here are consistent with these observations and confirm the need for surface treatment or matrix modification to improve fiber-matrix compatibility.

Overall, the microCT-based linear analysis provided a quantitative basis for understanding the weak adhesion and porosity concentration around the jute yarn. These interfacial features are likely to reduce mechanical performance and durability if not properly addressed through material design strategies. While the outer surface of the yarn appears to adhere partially to the cement paste, the presence of air voids suggests reduced interfacial bonding in that zone. Internally, the paste or mortar did not infiltrate the fiber structure, indicating a complete absence of penetration.

With the 3D analysis, it was possible to quantify the jute fiber with a volume of 54.60 mm^3 and a diameter distribution in the longitudinal direction with a maximum size of 1.60 mm; these results agree well with the evaluation of the linear measurements. The cement matrix has a total volume of 1129.16 mm^3

and a total percentage porosity of 4.30% with a pore distribution with a maximum diameter of the order of 1 mm.

Figure 6 presents the 3D analysis of the bioconcrete sample. The complete representation (Figure 6A) shows the cementitious matrix (gray), the matrix voids (blue), and the jute fiber (red) surrounded by a coating (beige). To highlight the distribution of voids around the coated fiber, the cementitious matrix was digitally removed in Figure 6B. The interface between the fiber and its protective layer is emphasized in Figure 6C, which displays the coated jute fiber, while Figure 6D shows the morphology of the isolated jute fiber. With deep learning segmentation, it was possible to distinguish in detail the different phases of bioconcrete with jute yarn, mainly in the region between the coating and jute fiber, as can be seen below in Figure 6.

4 | Conclusions

This study successfully leveraged x-ray computed microtomography (micro-CT) as a powerful non-destructive tool for thoroughly characterizing the microstructure and interfacial behavior of bioaggregates within cementitious matrices. The detailed 3D imaging capabilities of microCT proved invaluable in providing insights into complex interactions that are critical for the design of sustainable bioconcretes.

For bioconcrete incorporating macauba endocarp, micro-CT analysis revealed excellent interfacial adhesion, characterized by a notable absence of voids along the aggregate-matrix boundary. This superior bonding is attributed to the endocarp's low water absorption (~9% by weight), which is significantly lower than that of typical wood-based materials (150%–200%) [14]. This low water uptake minimized shrinkage-induced detachment, leading to improved dimensional stability and better compatibility within the cementitious matrix. Furthermore, microCT allowed for the visualization of the endocarp's intrinsic porous morphology, including germination pores and vascular channels, contributing to a comprehensive understanding of its properties.

In contrast, the analysis of the jute fiber bioconcrete highlighted distinct challenges at the interface. The images clearly depicted interface debonding, primarily due to the shrinkage of the jute fibers and the limited penetration of the cementitious matrix into the inner fiber bundles. While the outer filaments showed some partial adhesion, the internal regions remained largely unbonded, indicating issues with matrix infiltration. Despite these interfacial challenges, the study also demonstrated that jute textiles effectively absorbed and contained 102% of the phase change material (PCM) by weight within their capillary porosity, indicating their potential for thermal regulation applications.

Overall, the findings underscore the critical role of microCT in evaluating and understanding the complex interactions at the

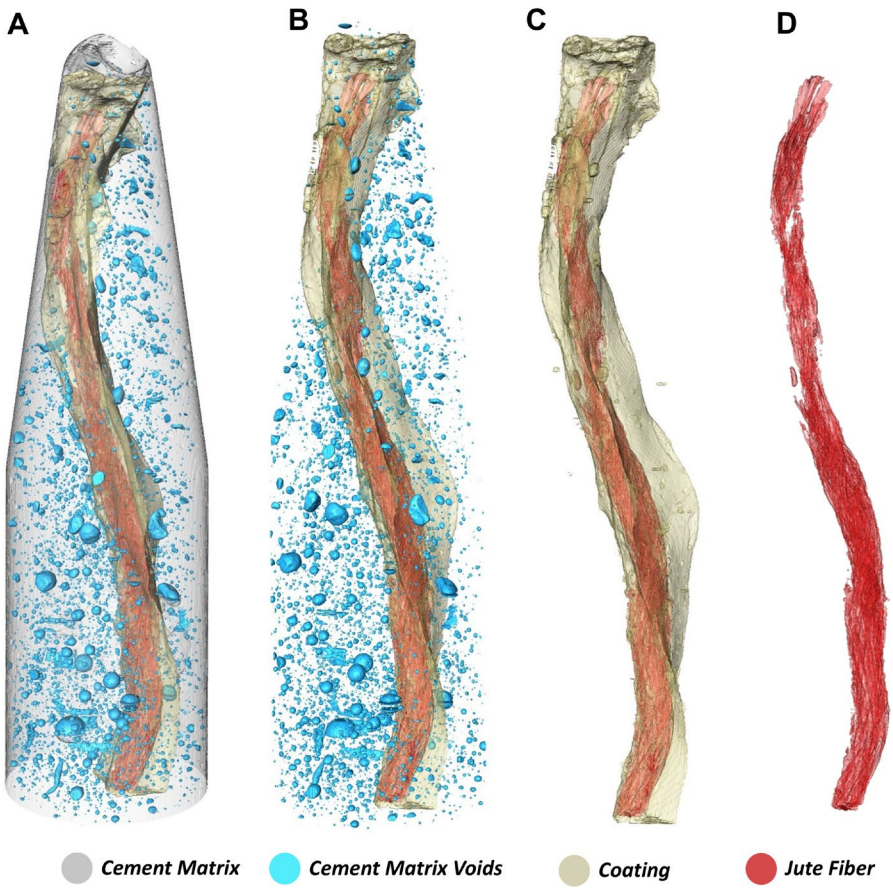


FIGURE 6 | MicroCT 3D analysis of jute fiber bioconcrete. (A) Full representation of the bioconcrete sample, showing the segmented phases. (B) Bioconcrete sample with the cement matrix removed to highlight the distribution of voids. (C) The coated jute fiber, emphasizing the interface. (D) The isolated jute fiber, providing a clear view of its morphology. [Colour figure can be viewed at wileyonlinelibrary.com]

cementitious matrix–bioaggregate interface. This advanced imaging technique provides essential microstructural information, enabling researchers to identify key factors influencing bond performance, porosity distribution, and material behavior, which are vital for optimizing the formulation and long-term durability of sustainable bioconcretes.

Acknowledgments

This study was financed in part by FAPERJ—Fundação Carlos Chagas Filho de Amparo à Pesquisa do Estado do Rio de Janeiro, through the Pós-Doutorado Nota 10 Fellowship (Grant No. SEI-260003/001101/2025 to O.M.O.A.), the National Council for Scientific and Technological Development—CNPq, INCT-INAIS (grant 406303/2022-3 and productivity fellowships 314225/2021 to R.T.L.). The Article Processing Charge for the publication of this research was funded by the Coordenação de Aperfeiçoamento de Pessoal de Nível Superior - Brasil (CAPES) (ROR identifier: 00x0ma614).

Conflicts of Interest

The authors declare no conflicts of interest.

Data Availability Statement

The data that support the findings of this study are available from the corresponding author upon reasonable request.

References

1. P. J. M. Monteiro, S. A. Miller, and A. Horvath, "Towards Sustainable Concrete," *Nature Materials* 16 (2017): 698–699, https://doi.org/10.1038/nmat4930.

2. A. Pokharel, K. J. Falua, A. Babaei-Ghazvini, and B. Acharya, "Biobased Polymer Composites: A Review," *Journal of Composites Science* 6, no. 9 (2022): 255, https://doi.org/10.3390/jcs6090255.

3. F. L. Santos, R. V. Pereira, F. Scinocca, C. M. F. Grupioni, and R. P. Castro, "Macauba Palm Endocarps Under Compression Forces Considering the Different Treatments: A Study About Physical and Mechanical Properties for Seed Extraction," *Industrial Crops and Products* 220 (2024): 119121, https://doi.org/10.1016/j.indcrop.2024.119121.

4. S. R. Ferreira, R. G. M. de Andrade, G. M. de Andrade, et al., "Bond Behavior of a Bio-Aggregate Embedded in Cement-Based Matrix," *Materials* 15 (2022): 6151, https://doi.org/10.3390/ma15176151.

5. G. M. de Andrade, R. G. M. de Andrade, O. M. O. de Araújo, R. T. Lopes, T. C. Guimarães, and S. R. Ferreira, "Performance of Concrete Containing *Acrocomia aculeata* Endocarp as Bioaggregate: An Experimental and Statistical Approach," *Construction and Building Materials* 417 (2024): 138667, https://doi.org/10.1016/j.conbuildmat.2024.138667.

6. T. Ashour, H. Wieland, H. Georg, et al., "Performance of Straw Bale Wall: A Case Study," *Energy and Buildings* 87 (2015): 146–152, https://doi.org/10.1016/j.enbuild.2011.04.001.

7. E. N. Landis and D. T. Keane, "X-Ray Microtomography," *Materials Characterization* 61 (2010): 1305–1316, https://doi.org/10.1016/j.matchar.2010.09.012.

8. J. L. Provis, R. J. Myers, C. E. White, et al., "X-Ray Microtomography Shows Pore Structure and Tortuosity in Alkali-Activated Binders," *Cement and Concrete Research* 68 (2015): 24–33, https://doi.org/10.1016/j.cemconres.2012.03.004.

9. T. De Kock, M. A. Boone, T. De Schryver, et al., "A Pore-Scale Study of Fracture Dynamics in Rock Using X-Ray Micro-CT Under Ambient Freeze-Thaw Cycling," *Environmental Science & Technology* 54 (2020): 6944–6954, https://doi.org/10.1021/es505738d.

10. D. Zhou, C. Y. Zhao, and Y. Tian, "Review on Thermal Energy Storage With Phase Change Materials (PCMs) in Building Applications," *Applied Energy* 92 (2012): 593–605, https://doi.org/10.1016/j.apenergy.2011.08.025.

11. T. C. Guimarães, M. C. Dias, O. M. O. de Araújo, et al., "The Influence of Cellulose Microcrystals and Nanofibrils in XSBR Polymers on the Mechanical Properties of Jute Textile-Reinforced Cementitious Composites," *Cellulose* 31 (2024): 3961–3979, https://doi.org/10.1007/s10570-024-05810-2.

12. R. Lorenzoni, S. Paciornik, F. A. Silva, and G. Bruno, "MicroCT and 3D Image Processing and Analysis to Investigate Strain-Hardening Cement-Based Composites (SHCC)," in *Strain Hardening Cementitious Composites*, ed. M. Kunieda (Springer, 2023), 171–182, https://doi.org/10.1007/978-3-031-15805-6_13.

13. J. F. Natalli, E. C. S. Thomaz, J. C. Mendesa, and R. A. F. Peixoto, "A Review on the Evolution of Portland Cement and Chemical Admixtures in Brazil," *Revista IBRACON de Estruturas e Materiais* 14 (2021): e14005, https://doi.org/10.1590/S1983-41952021000600003.

14. S. R. Ferreira, M. Pepe, E. Martinelli, F. de Andrade Silva, and R. D. Toledo Filho, "Influence of Natural Fibers Characteristics on the Interface Mechanics With Cement Based Matrices," *Composites. Part B, Engineering* 140 (2018): 183–196, https://doi.org/10.1016/j.compositesb.2017.12.016.

15. K. L. Scrivener, V. M. John, and E. M. Gartner, "Eco-Efficient Cements: Potential Economically Viable Solutions for a Low-CO_2 Cement-Based Materials Industry," *Cement and Concrete Research* 114 (2018): 2–26, https://doi.org/10.1016/j.cemconres.2018.03.015.

16. H. Bao, G. Xu, M. Yu, et al., "Evolution of ITZ and Its Effect on the Carbonation Depth of Concrete Under Supercritical CO_2 Condition," *Cement and Concrete Composites* 126 (2022): 104336, https://doi.org/10.1016/j.cemconcomp.2021.104336.

17. L. Sun, C. Yao, A. Guo, and Z. Yu, "A Review on the Application of Lignocellulosic Biomass Ash in Cement-Based Composites," *Materials* 16, no. 17 (2023): 5997, https://doi.org/10.3390/ma16175997.

18. L. D. O. Menali, U. L. Zidanes, M. C. Dias, et al., "Production and Analysis of the Physical and Mechanical of Particleboards Panels Produced With *Acrocomia aculeata* Endocarp," *Cerne* 30 (2024): e-103302, https://doi.org/10.1590/01047760202430013302.

Supporting Information

Additional supporting information can be found online in the Supporting Information section. **Video S1:** 3D visualization of the microstructure of a cementitious composite with jute fiber, obtained by X-ray microtomography (microCT). The animation demonstrates the segmentation of the material's different phases, performed using a deep learning-based methodology. The composite's layers are progressively and digitally removed to allow for a detailed analysis of the interaction between the components, as shown in Figure 6 of the manuscript.